Article

Probing Gluons with the Future Spin Physics Detector

Alexey Guskov [1], Amaresh Datta [1,*], Anton Karpishkov [1,2], Igor Denisenko [1] and Vladimir Saleev [1,2]

[1] Joint Institute for Nuclear Research (JINR), Joliot-Curie 20, Dubna 141980, Russia; avg@jinr.ru (A.G.); karpishkoff@gmail.com (A.K.); iden@jinr.ru (I.D.); vasaleev@mail.ru (V.S.)

[2] Department of General and Theoretical Physics, Samara National Research University, 34, Moskovskoye Shosse, Samara 443086, Russia

[*] Correspondence: amareshdatta@gmail.com

Abstract: In this paper, we review the physics studies to be performed with the Spin Physics Detector (SPD) at the Nuclotron-based Ion Collider fAcility (NICA) which is a multi-purpose experiment designed to study nucleon spin structure in the three dimensions. With capabilities to collide polarized protons and deuterons with center-of-mass energy up to 27 GeV and luminosity up to 10^{32} cm^{-2} s^{-1} for protons (an order of magnitude less for deuterons), the experiment is considered to allow measurements of cross-sections and spin asymmetries of hadronic processes sensitive to the unpolarized and various polarized (helicity, Sivers, Boer-Mulders) gluon distributions inside the nucleons. Results from the SPD will be complimentary to the present high-energy spin experiments at the RHIC (Relativistic Heavy Ion Collider) facility or future experiments such as the Electron-Ion Collider (EIC) at BNL (Brookhaven National Laboratory) and the AFTER experiment at the LHC (Large Hadron Collider) in understanding the spin structure of the basic building blocks of visible matter. Monte Carlo simulation-based results presented here demonstrate the impact of the SPD asymmetry measurements on gluon helicity parton distribution function (PDF) and gluon Sivers functions. With polarized deuteron collisions, the SPD is expected to be the unique laboratory for probing tensor-polarized gluon distributions. Additionally, there are possibilities of colliding other light nuclei, such as carbon, at reduced collision energy and luminosity during the first stage of the experiment.

Keywords: spin physics; nucleon spin; gluon helicity PDF; transverse momentum dependent (TMD) PDF; gluon Sivers function

1. Introduction

Over the last few decades, experimental results have often surprised the physics community and opened up new windows into the intricate details of the structure of the fundamental building blocks of nature. Results from the European Muon Collaboration (EMC) [1] have shed light on the importance of possible gluonic contributions to the nucleon spin. The findings from E704 experiment and other studies [2,3] regarding large single spin asymmetries have inspired the community to consider the motions of quarks and gluons within nucleons.

Visible matter made of quarks and gluons is mostly described by quantum chromodynamics (QCD), the theory of the strong force. The present understanding of quarks and gluons comes from the high energy limit of perturbative QCD (pQCD) [4,5]. Decades of experimental measurements of inclusive and semi-inclusive deep inelastic scattering (DIS) (at COMPASS and HERMES experiments), electron–positron scattering (at HERA accelerator), and hadron scattering (at Relativistic Heavy Ion Collider, RHIC), have provided us with a fairly precise description of quarks [6–8] within nucleons, using pQCD as the preferred tool for interpretations. However, the gluonic component (which accounts for about 99% of all nucleon mass and, therefore, all visible matter) is still to be understood.

It is imperative for the physics community to experimentally access the gluons inside the nucleons to consistently describe baryonic matter and its interactions.

Gluon distributions inside nucleons are harder to access compared to those of quarks in the semi-inclusive DIS scattering of leptons off hadrons. This is because gluons do not interact with leptons directly through the strong force. In recent years, high-energy hadronic scattering has been the best tool for probing the spin distributions of gluons within protons [9]. The understanding of gluon helicity distributions has changed over the first couple of decades of the twenty-first century as the analyses have included more experimental data from various sources [10–13].

A more complete picture of the three-dimensional partonic structure has emerged [14] in the last decade, along with more data available to access the transverse momentum dependent (TMD) parton distribution functions (PDFs). Large transverse asymmetries in hadron production have necessitated a closer look at the partonic structure, including transverse momentum-dependent distribution functions [15] and fragmentation [16].

The future Spin Physics Detector SPD [17] is an experiment proposed at the Nuclotron-based Ion Collider fAcility (NICA) located at the Joint Institute for Nuclear Research (JINR) in Dubna, Russia. It is particularly focused on probing the gluons inside protons and deuterons. The SPD is designed to allow cross-section and asymmetry measurements of several hadronic processes that are sensitive to various (unpolarized and polarized) gluon distributions.

The SPD is planned to operate at medium energy ranges (up to 10 GeV in the initial stage and up to 27 GeV in the later stage) that are complementary to the present and future experiments (Figure 1a) with higher center-of-mass energies (PHENIX, STAR, AFTER [18], and LHCspin [19] experiments). As a consequence, measurements at the SPD to probe high momentum fractions, x, and low-to-medium energy scales, Q^2, that will provide access to gluonic distribution in a kinematic regime (illustrated by Figure 1b) that is complementary to those accessed in other upcoming major spin physics experiments, such as the Electron Ion Collider (EIC) [20,21].
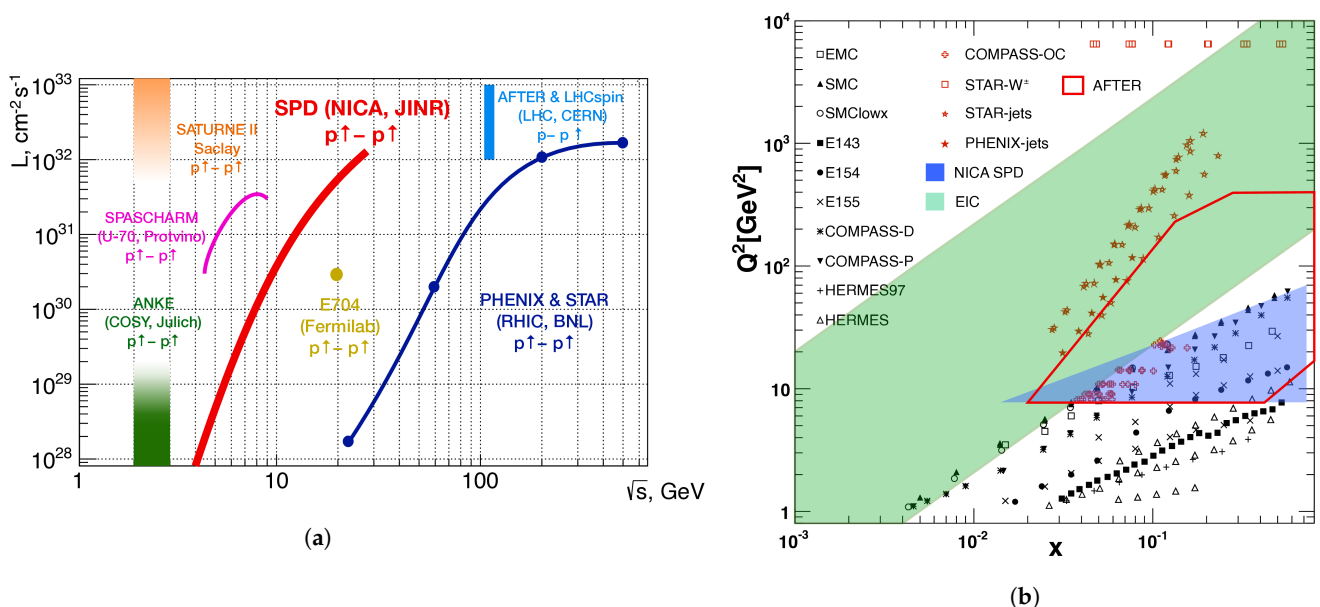

(a)

(b)

Figure 1. (**a**) Luminosity as a function of the center-of-mass energy of collision and (**b**) the kinemtic coverage for the Spin Dtector Physics (SPD) and other future spin experiments.

2. Physics and Detector Description

2.1. Physics of Stage I

In its initial stage, NICA is designed to offer proton beams of up to 5 GeV with a collision luminosity of up to 10^{31} cm^{-2}s^{-1} for the proton-proton (pp) collisions and up to 4.5 GeV/N (per nucleon) deuteron beams with collision luminosity of up to 10^{30} cm^{-2} s^{-1}

for the first few years. There are also possibilities of asymmetric collisions, such as proton-deutron (pd) and light nuclei (i.e., C, Ca) collisions.

The SPD is planned to take an advantage of the low energies at the initial stage to look for compelling and interesting physics effects in pp, dd, and possibly in the light nuclei collisions. Various physics goals and programs for this initial stage are discussed in detail in Ref. [22].

2.1.1. Spin Effects in Elastic Collisions

Measurements of the elastic scattering cross-sections for pp collisions at small angles, $\theta \sim 3$–$10°$, provides an access to a kinematic region with momentum transfer, $|t| \sim 0.1$–$0.8\,\text{GeV}^2$. Small oscillations in the t-dependence probe the proton structure involving mesons in the periphery (pion cloud model). The SPD is expected to provide high-precision data in this region to test models of the two-pion exchange process in elastic scattering.

Glauber models with Gribov inelastic corrections have been successful [23] add. in describing elastic dd scattering data at energies ranging from a few tens of GeV. At the first stage, energies of up to the collision center-of-mass energy, $\sqrt{s} = 9\,\text{GeV}/N$, for unpolarized dd cross-section measurements and subsequent comparisons with calculations to test if the inelastic corrections are relevant for this kinematic regime.

At large angles $\theta \sim 90°$, dd $\to$ dd processes are sensitive to the six-quark structures of the deuterons. The SPD is designed to provide with cross-section measurements of dd elastic collisions at large center-of-mass angle, θ_{CM}, to search for non-nucleonic degrees of freedom.

2.1.2. Charmonium Production

The SPD is considered to measure light and charm meson productions near the production threshold. Of particular interest is the charmonium (J/Ψ) formation near the threshold for pp and dd collisions as the charmonium formation tests the isotopic dependence (involvement of protons or neutrons) on the production due to the different spin structures of the corresponding matrix elements.

The threshold production of charmonia in ion–ion collisions is also a promising probe of the quark–gluon plasma (QGP).

2.1.3. Strange Hypernuclei Production

Although there has been no evidence of stable hypernuclei of a baryon number, $A = 2$, the measurements exist [24] of candidates ($^3_\Lambda$He, $^3_\Lambda$H) with a baryon number, $A = 3$. Proposals have been made to look for the neutral hypernucleus $^4_{\Lambda\Lambda}n$ in the dd collisions at the SPD. Calculations predict [22] a peak in the production at $\sqrt{s} = 5.2\,\text{GeV}$. A measurement of this hypernucleus with a strangeness value of $S = -2$ would be the first of this kind.

2.1.4. Other Interesting Physics at Stage I

Measurements during stage I of the SPD are also considered to test various effects that can be broadly categorized as multiquark correlations. These include nuclear PDFs involving fluctons or multiquark degrees of freedom, higher twist contributions of two or three quark correlations in PDFs, multi-parton scattering in hadronic and nuclear collisions, and the formation of exotic multiquark resonance states, i.e., tetraquark and pentaquark.

2.2. Physics of Stage II

For stage II, when NICA is foreseen to reach its full potential (Figure 2a), in terms of luminosity ($10^{32}\,\text{cm}^{-2}\,\text{s}^{-1}$) for pp collisions, as well as energy and polarization capacities, the SPD is planned to primarily focus on making measurements of observables from polarized pp and dd collisions that are sensitive to the gluon distributions inside nucleons (Figure 2b). Detailed discussions regarding the access to gluon contents through measurements at the SPD can be found in Ref. [25]. At peak luminosities, one year of data collected at the SPD is

expected to correspond to the integrated luminosities of 1.0 and 0.1 fb^{-1} for pp collisions at $\sqrt{s} = 27$ and 13.5 GeV, respectively.

(a)
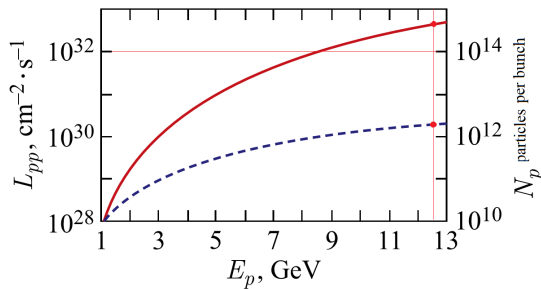
	Unpolarized	Circular	Linear
Unpolarized	g(x) density		$h_1^{\perp g}(x, k_T)$ Boer-Mulders function
Longitudinal		$\Delta g(x)$ helicity	Kotzinian-Mulders function
Transverse	$\Delta_N^g(x, k_T)$ Sivers function	Worm-gear function	$\Delta_T g(x)$ transversity (deuteron only), pretzelosity

(b)

Figure 2. (**a**) Expected luminosity, L_{pp}, and bunch intensity, N_p, as a function of proton beam energy, E_p, at NICA facility. (**b**) Parton density functions (PDFs) (in red) to be accessed at the SPD.

Measurements of asymmetries and correlations from polarized pp collisions at the SPD is considered to be, in particular, sensitive to gluon helicity, Sivers, and Boer–Mulders distributions. Measurements from the polarized deuteron collisions access gluon transversity and tensor-polarized gluon distributions inside deuterons. NICA is designed to be the first facility to provide polarized deuteron beams in such energy ranges and the SPD is expected to have the unique ability to access quantities that have not been measured before.

Unpolarized cross-section measurements at the SPD is expected to provide the data that are sensitive to the unpolarized gluon distributions, $g(x)$. Double-helicity asymmetry measurements, A_{LL}, at the SPD probe the gluon helicity distribution function, $\Delta g(x)$; single transverse spin asymmetries, A_N, provide access to the gluon Sivers function, $\Delta_N^g(x, k_T)$; and measurements of azimuthal correlations in hadron pair production from unpolarized pp collisions probe the Boer–Mulders distributions, $h_1^{\perp}(x, k_T)$. Double and single vector/tensor asymmetries from polarized dd collisions probe, respectively, the gluon transversity, $\Delta g_T(x)$, and tensor-polarized gluon PDF, $C_G^T(x)$.

2.3. Detectors for Stage I

The SPD detector system [26] is designed to have complete 4π coverage at a solid angle. The design includes a barrel part and two endcaps. In the barrel part, the SPD features a solenoid magnet, providing a field of up to 1.2 T at the interaction point. The magnetic field provides charge separation for particle tracks and aids in determining the momentum of charged particles.

Moving outward from the aluminum beam pipe, the detectors in the barrel part of the SPD at this stage is planned to include the following subsystems (Figure 3):

1. A Micromegas tracker that helps in the charged particle momentum reconstruction.
2. A multi-layer tracker system with PET (metal-coated polyethylene terephthalate) straws arranged along Z, U, and V (U and V are stereo layers at 5° with Z straws along the beam direction) with a spatial resolution of about 150 μm. The tracker will provide charged particle momentum as well as limited particle identification using energy depositions, $-dE/dx$, in the straw layers with an energy resolution, $\delta E/E = 8.5\%$.
3. A range system (RS) just outside of the magnet, consisting of layers of mini drift tubes (MDTs) and absorbing material (Fe), is designed to provide muon-to-hadron separation of the charged tracks and hadronic calorimetry.

Each side of the endcaps of the SPD detector system in stage I is designed to consist of the Micromegas, straw tracker, beam–beam counter (BBC) to provide local polarimetry, luminosity control, collision timing information, range system, and zero-degree calorimeter (ZDC) at small polar angles providing local polarimetry, luminosity control, and event selection criteria for elastic collisions.
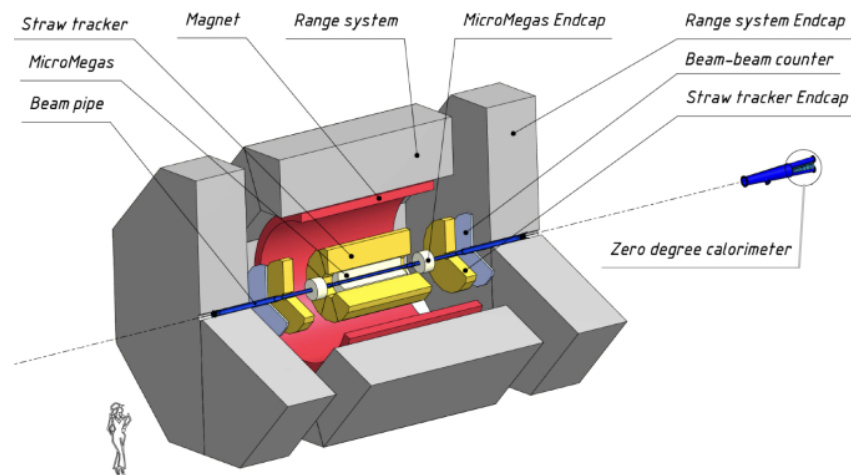
Figure 3. Schematic of the SPD detector at stage I.

2.4. Detectors for Stage II

For the second stage of the operations, due to different requirements of the physics in focus at this stage, some parts to be replaced and new detectors to be included [26].

For stage II, the barrel part of the SPD to consist of (Figure 4):

1. An improved silicon vertex detector to replace the Micromegas from stage I. Two options being considered are the (1) monolithic active pixel sensor (MAPS) and (2) double-sided silicon strip detector (DSSD). The new component is designed to contribute to tracking, momentum determination, and reconstructing secondary vertices for the decays of short-lived particles. The MAPS silicon tracker to provide a secondary vertex position resolution of 40–60 μm.
2. A straw tracker. The tracking system is designed to provide a transverse momentum resolution, $\delta p_T / p_T = 2\%$ for tracks with a transverse momentum of 1 GeV/c, with c the speed of light (the same resolution in stage I).
3. A time-of-flight (TOF) detector for particle identification, with a timing resolution of 50 ps and π/K separation of charged tracks with momenta up to 1.5 GeV/c.
4. An electromagnetic calorimeter to determine photon energies, with an energy resolution, $\delta E / E = 5\% / \sqrt{E} \oplus 1\%$, and the identification of electrons and positrons.
5. Range system.

The endcaps are designed also to have some new components, i.e., a silicon vertex detector, straw tracker, BBC, TOF detector, aerogel detector to extend the π/K separation up to 2.5 GeV/c momentum, electromagnetic calorimeter, and a ZDC.
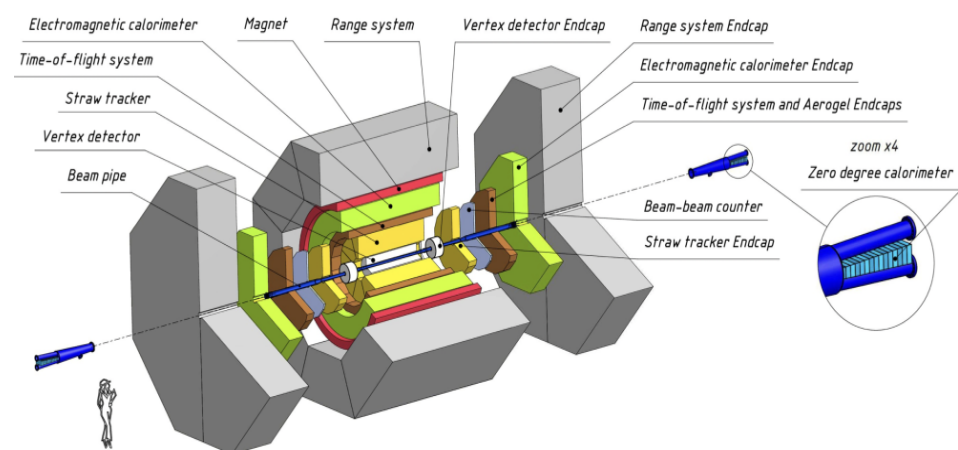

Figure 4. Schematic of the SPD detector at stage II.

2.5. Detector Performance

Figure 5 shows the Monte Carlo simulation performances of some of the detectors used in the key measurements. From the left, in Figure 5a, the two-photon invariant mass spectra using the electromagnetic calorimeter demonstrate the pion mass resolution, $\delta_m = 9.8$ MeV, that can be achieved. Figure 5b illustrates the particle identification using the time-of-flight detector. Pion–kaon separation can be achieved for particle momentum of up to 1.5 GeV/c. Figure 5c illustrates the secondary vertex resolution along the beam direction for three possibilities of central tracking detectors, i.e., Micromegas for the first stage and DSSD or MAPS for the second stage. MAPS-based detectors are widely recognized as the best-performing detectors, providing secondary vertex position resolutions, $\delta_z \sim 50$ μm.

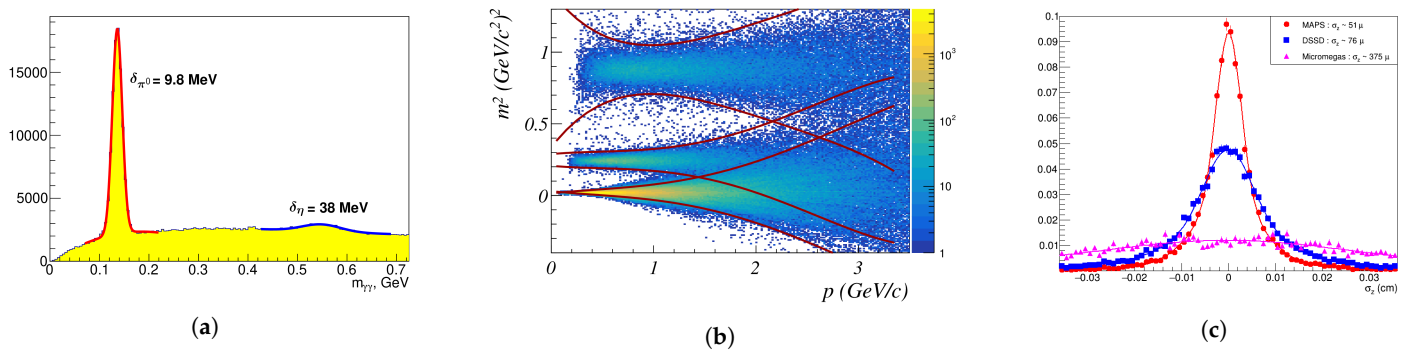(a) (b) (c)

Figure 5. (**a**) Mass resolution of pion mass reconstruction from two photons, (**b**) mass-squared versus momentum at the time-of-flight detector, and (**c**) D^0 secondary vertex resolution along the beam direction for three different options of vertex detectors.

3. Monte Carlo Studies

In order to access various gluon distributions, the SPD to focus on processes involving gluonic interactions. Three major channels of interest at the SPD are (Figure 6):

- Quark–gluon scattering to prompt photons (Figure 6a). This is a particularly clean channel for theoretical interpretations as it does not involve hadronization.
- Gluon fusion to charmonia production (Figure 6b) (J/Ψ, $\Psi(2S)$, $\chi_{c1/c2}$). Measurements at the SPD to primarily focus on utilizing dimuon decay channels of charmonia.
- Gluon fusion to open-charm mesons (Figure 6c). D mesons at the SPD are considered to be detected via hadronic decay channels. This is the highest statistics channel but a challenging measurement due to the large amount of combinatorial backgrounds.
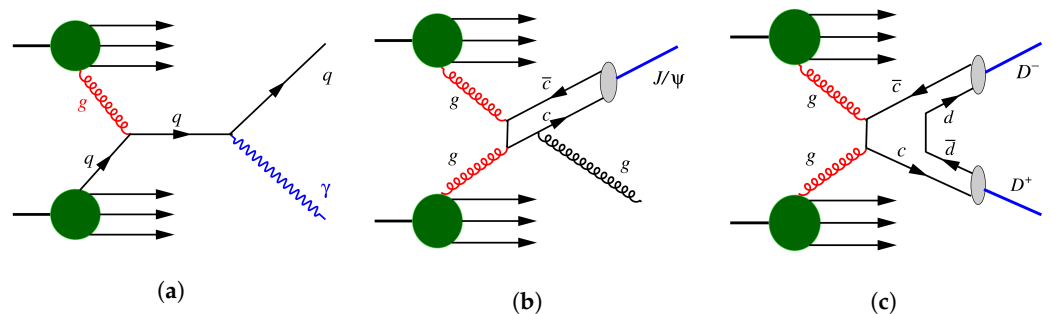

(a) (b) (c)

Figure 6. Schematics of partonic sub-processes of interest: (**a**) quark–gluon scattering to prompt photon production, (**b**) gluon fusion resulting in charmonia production, and (**c**) gluon fusion leading to open-charm production.

As illustrated in Figure 7, at the peak SPD energy of $\sqrt{s} = 27$ GeV, open-charm processes are the most abundant among these three. However, the hadronic channels of charmed meson decays are notoriously complicated to be measured because of the significantly higher levels of combinatorial backgrounds arising from random combinations

of hadrons from other hard processes. Charmonia are comparatively easier to be measured via dimuon decay channels with good muon–hadron separation (using the range system at the SPD). Prompt photons, while the rarest among these processes, have the advantage of being the cleanest probes for theoretical interpretations. This channel also requires a careful estimation of backgrounds arising from the decays of light-neutral mesons such as π^0 and η.
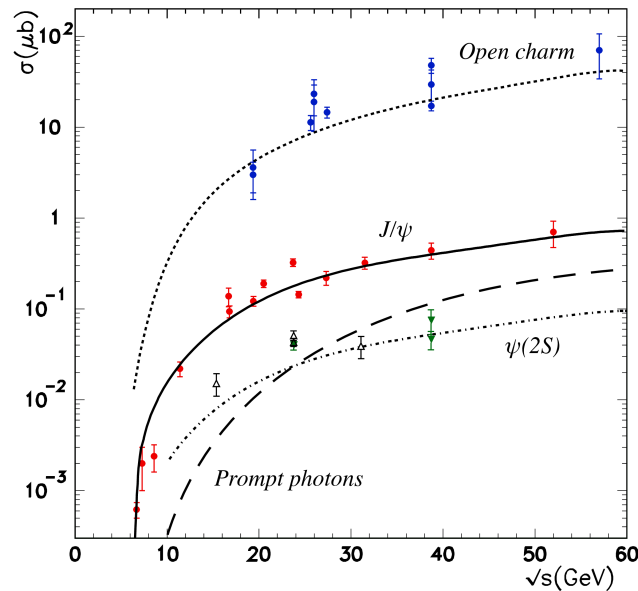

Figure 7. Center-of-mass energy dependence of cross-sections of the three channels of interest at SPD kinematics [25]. Adapted from Ref. [27] (with permission of *The European Physical Journal*).

3.1. Prompt Photon Measurements

Prompt photon productions in the leading order may occur via the Compton scattering of a gluon and quark–antiquark ($q\bar{q}$) annihilation. However, at SPD energies, the $q\bar{q} \rightarrow g\gamma$ contribution is small. The fragmentation contribution (from scattered (anti-)quarks) to prompt photon production is also estimated to be small (15–30%) [25]. This makes prompt photons a most suitable tool for probing the gluon distributions inside nucleons. The measurements are planned to be performed using the electromagnetic calorimeter, and the photons from neutral light meson (i.e., π^0 and/or η) decays are the largest background sources. Untagged photons from π^0 can be estimated using Monte Carlo simulations.

The double-helicity asymmetry, A_{LL}^{γ}, of the prompt photons at the SPD is sensitive to the gluon distribution in the high momentum fraction range. In Ref. [28], the inclusion of new measurements has been tested with Monte Carlo reweighting instead of the full extraction of PDFs, creating an efficient technique to estimate the impact of new data points on a global analysis of PDF extraction. A similar study (courtesy of W. Vogelsang, R. Sassot, I. Borsa), utilizing the NNPDF3.0 unpolarized [8] and DSSV14 polarized [9] PDF sets, has estimated the impact of the A_{LL}^{γ} measurement with the projected statistical uncertainties (Figure 8), considering one year of recorded data expected at the SPD. Figure 9 shows that in the high-x region, $0.2 \leq x \leq 0.8$, SPD measurements can be used to reduce the uncertainties of the gluon helicity distribution, $\Delta g(x)$, by a factor of about 2.
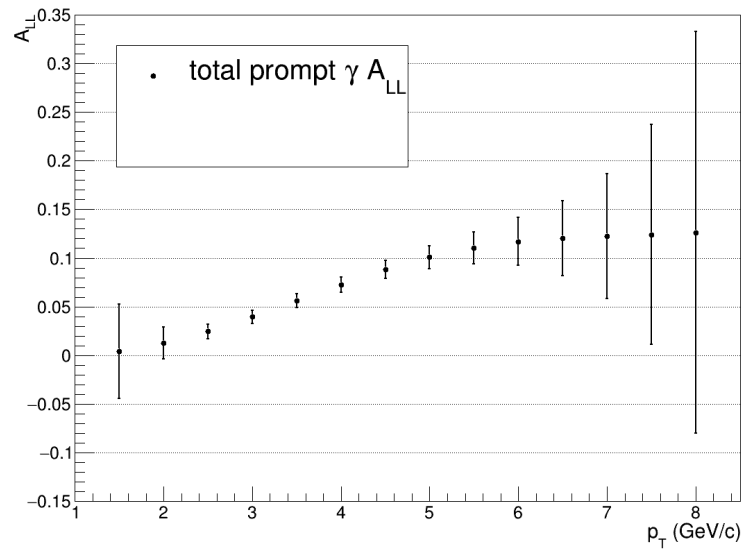
Figure 8. Prompt photon double-helicity asymmetry as a function of transverse momentum calculated using the NNPDF3.0 unpolarized [8] and DSSV14 polarized [9] PDF sets, taking into account the projected uncertainties from measurements based on one year of the data expected at the SPD.
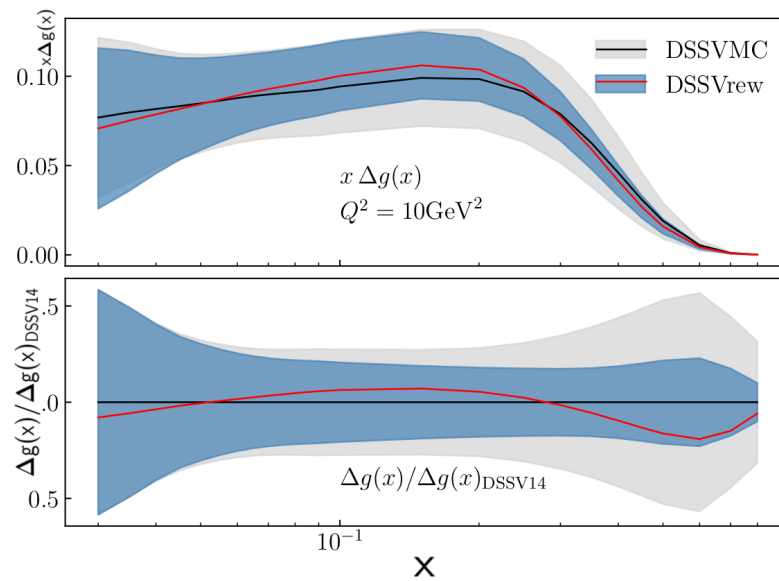

Figure 9. Estimated impact of prompt photon double-helicity asymmetry measurements at the SPD on the gluon helicity distribution function, $\Delta g(x)$. The black and red solid lines represent the mean values of a thousand replicas of the DSSV14 polarized gluon PDF [9], before and after reweighting using the projected SPD measurements, respectively. The gray and light blue bands represent the corresponding standard deviation uncertainties.

Theoretical estimates of the single transverse spin asymmetries show (see Figure 10a) that the asymmetries in the forward x_F-region are dominated by the quark–antiquark annihilation process, whereas the gluon-dominated process generates asymmetries in the backward x_F-region; here, x_F is the Feynman x. Figure 10b shows contribution of the background from neutral pion decays to the uncertainties in the planned measurements.
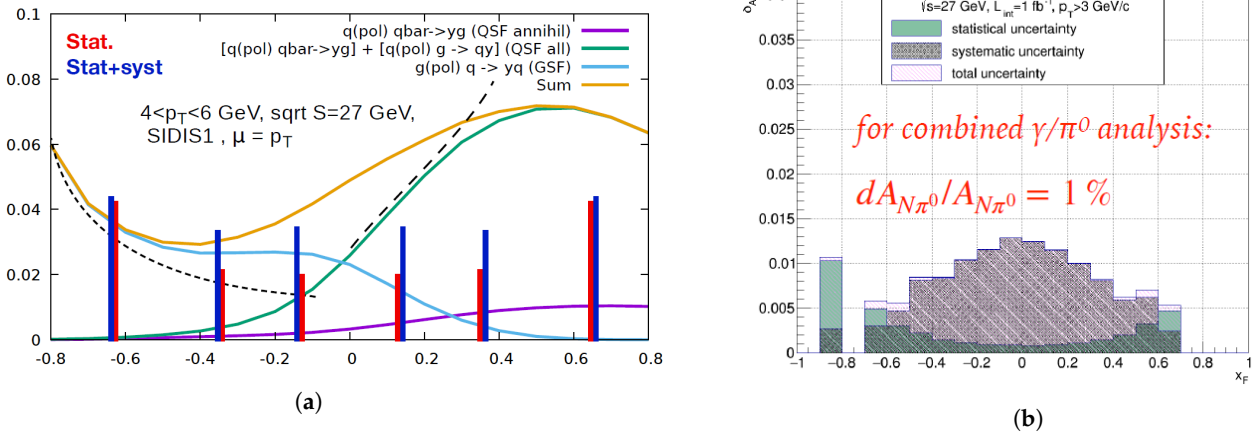
(a)

(b)

Figure 10. (a) Theoretical estimates of A_N^γ for the SPD. Calculations are performed using SIDIS1 parameterization [29] of the gluon Sivers function (GSF) and quark Sivers function (QSF). The dashed lines are twist-3 predictions for $\sqrt{s} = 30$ GeV and $p_T = 4$ GeV/c for negative and positive values of x_F. Red and blue vertical lines illustrate the statistical and combined (statistical + systematic) uncertaines from future SPD data for one year. (b) Estimated uncertainties for the single transverse spin asymmetry, A_N^γ, as functions of the Feynman x, x_F.

3.2. Charmonia Measurements

The charmonia production at the SPD energies (10–27 GeV) is expected to be dominated by the gluon–gluon fusion process [25]. The charmonia measurement via the dimuon invariant mass spectra, using the range system as the muon identifier, is expected to be a powerful tool at the SPD. The mass resolution of ~40 MeV, or better, is expected for J/Ψ from the dimuon invariant mass spectra.

In total, about 12 M events with J/Ψ are expected from one year of data to be collected at the peak luminosity of the SPD [25]. It will also be possible to perform measurements involving rarer charmonia. $\Psi(2S)$ can be detected via $\mu^+\mu^-$ and $\mu^+\mu^-\pi^+\pi^-$ decay channels. About 700,000 events producing $\Psi(2S)$ are expected from one year of data at the SPD. Moreover, χ_{c1} and χ_{c2} can be measured via the $\gamma\mu^+\mu^-$ channel; about 2.5 M events, including both types, are expected in one year of data at the peak luminosity. The characteristic plots are shown in Figure 11.
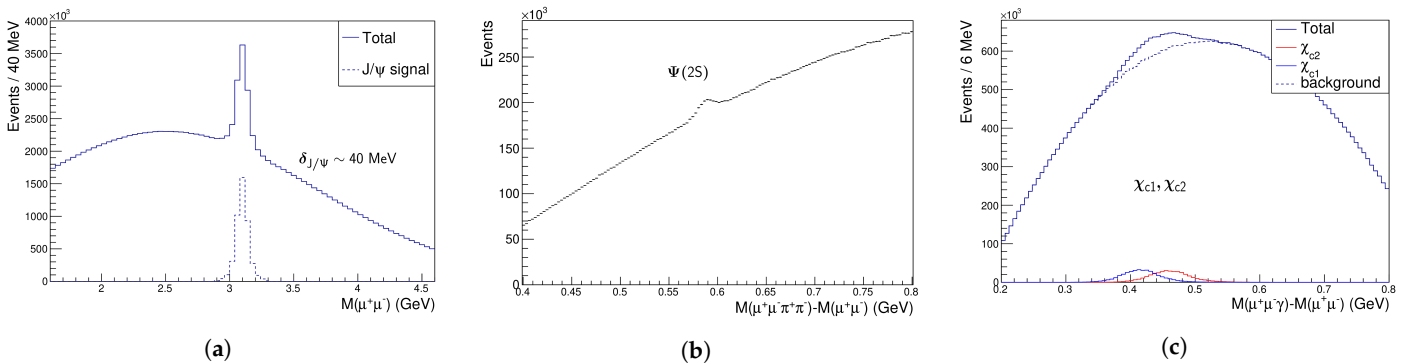

(a)

(b)

(c)

Figure 11. Monte Carlo simulation for the SPD: (a) dimuon invariant mass spectra for J/Ψ measurements; (b) invariant mass spectra for $\Psi(2S)$ measurements; (c) invariant mass spectra with the $\chi_{c1/c2}$ peaks indicated.

Alongside the unpolarized cross-section, which can be used to compare with theoretical estimations to shed light on the poorly understood hadronization models of charmonia, the double-helicity asymmetry, A_{LL}, and single transverse spin asymmetry, A_N, to be measured as well. It is expected that the possible high-precision $A_{LL}^{J/\Psi}$ measurements at the SPD will improve the current understanding of the gluon helicity PDF. Figure 12a

represents the expected statistical uncertainties of the double-helicity asymmetry of J/Ψ at the SPD for three different selection criteria for the polar angle of the muons from J/Ψ decays.
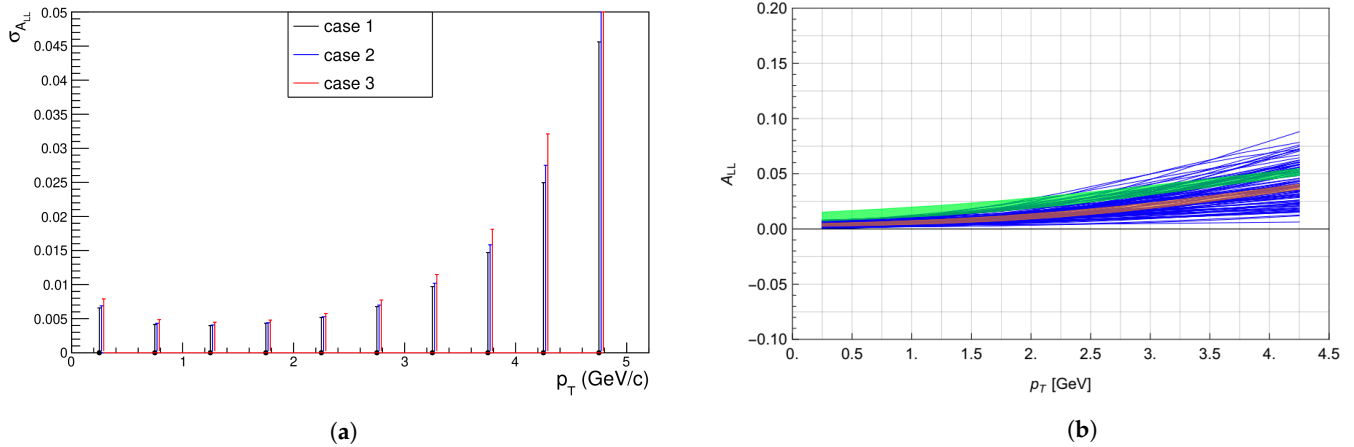

(**a**)

(**b**)

Figure 12. (**a**) Projected statistical uncertainties of $A_{LL}^{J/\Psi}$ for three different cases of selection cuts on the muon polar angles are shown. (**b**) Estimated $A_{LL}^{J/\Psi}$ as a function of p_T calculated using unpolarized NNPDF NLO [8] and polarized NNPDFpol1.1 [7] sets. The green band indicates uncertainties due to hadronization parameters and the brown band indicates scale uncertainties.

In a recent simulation study, performed for the work presented here, $A_{LL}^{J/\Psi}$ was calculated (Figure 12b) using NNPDF NLO unpolarized [8] and NNPDFpol1.1 polarized [7] sets. Using a technique similar to that of Ref. [28], the resulting calculations of $A_{LL}^{J/\Psi}$ are used, along with the projected uncertainties at the SPD for one year of data expected, to reweight the polarized PDF replicas; this technique is employed to estimate the impact of the measurement at the SPD. Figure 13 illustrates the impact of J/Ψ double-helicity asymmetry for the future measurements at the SPD. Expected measurements will significantly reduce uncertainties in the Bjorken-x range of $0.2 \leq x \leq 0.5$.
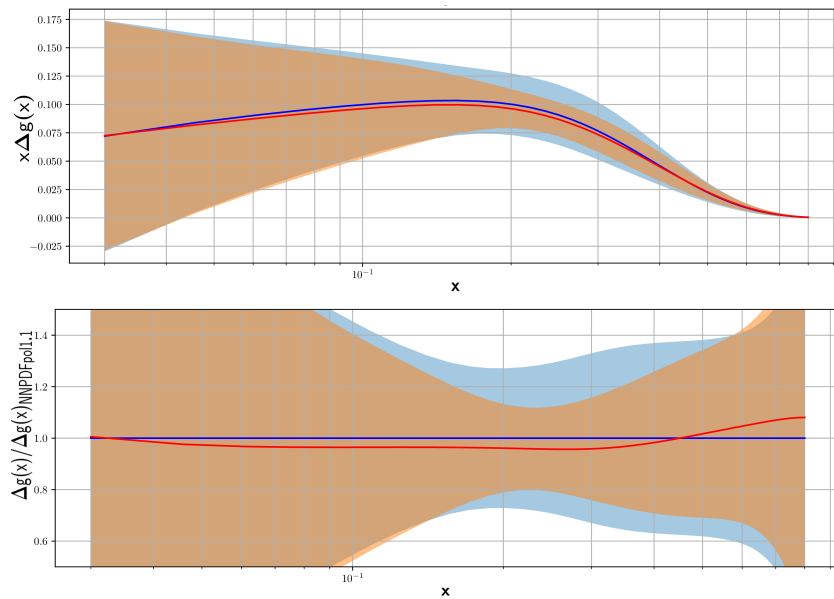

Figure 13. Estimated impact of double-helicity asymmetry measurementes of J/Ψ at the SPD on the gluon helicity distrbution function, $\Delta g(x)$. Blue and red lines show the mean of the NNPDFpol1.1 [7] replica sets before and after the reweighting, respectively, using the projected uncertainties for the future SPD measurements. Light blue and light orange bands show the corresponding standard deviation uncertainties.

Single transverse spin asymmetries of J/Ψ are sensitive to the gluon Sivers distributions. Theoretical estimations [30] of the $A_N^{J/\Psi}$ strongly depend on the choice of the parton models as well as on hadronization models. Estimations may differ by an order of magnitude, depending on the phenomenological parameterization used, as shown in Figure 14. High-precision measurements of $A_N^{J/\Psi}$ can be especially useful in reducing the model dependence in the SPD kinematic regime.
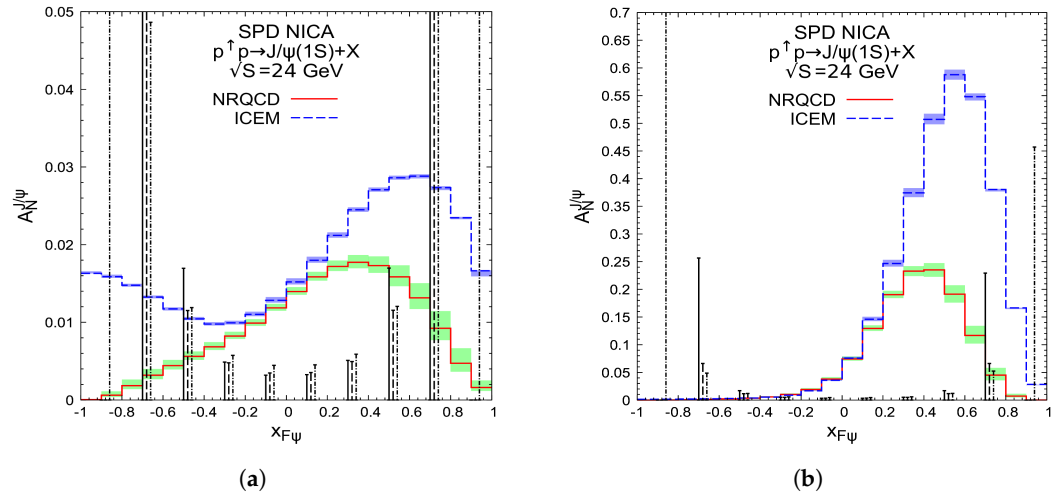

(a)   (b)

Figure 14. Estimated single transverse spin asymmetries of J/Ψ as functions of x_F using two different parameterizations of the gluon Sivers function: (**a**) D'Alesio et al. [31] and (**b**) SIDIS1 [29]. In both cases, (**a**,**b**), the calculations are performed for two different models for J/Ψ formation, namely, the non-relativistic QCD (NRQCD) and improved colour evaporation model (ICEM) [30]. Green and blue bands represent scale uncertainties in the theoretical calculations. Projected statistical uncertainties (for three different selection cuts on the muon polar angles) for one year of expected data at the SPD are shown as vertical lines.

3.3. Open-Charm Measurements

Open-charm meson spin asymmetries have been measured in DIS experiments, such as COMPASS [32], which has been used to estimate gluon polarization, but it has not been measured as yet in pp collider experiments. At the SPD, open-charm D mesons are expected to be detected through hadronic decay channels, such as $D^0 \to \pi^+ K^-$, $D^+ \to \pi^+ \pi^+ K^-$, and the antiparticle counterparts. Figure 7 shows that the open-charm production cross-sections are almost two orders of magnitude larger than charmonium production cross-sections, contributing to their abundance in the context of the SPD kinematics. However, the abundance of charged pions and kaons from other hard-scattering processes makes it a particularly challenging measurement. The combinatorial background from pions and kaons from other processes is more than four orders of magnitude larger than the signal.

Theoretical calculations of the single transverse spin asymmetry for inclusive D mesons at the SPD kinematics (Figure 15) using the colour gauge–invariant generalized parton model (CGI-GPM) show significant expected asymmetries in the forward region ($x_F > 0.2$); for backward x_F, the asymmetry is compatible with zero. However, the size of the asymmetry depends strongly on the parameterization used for the parton model.
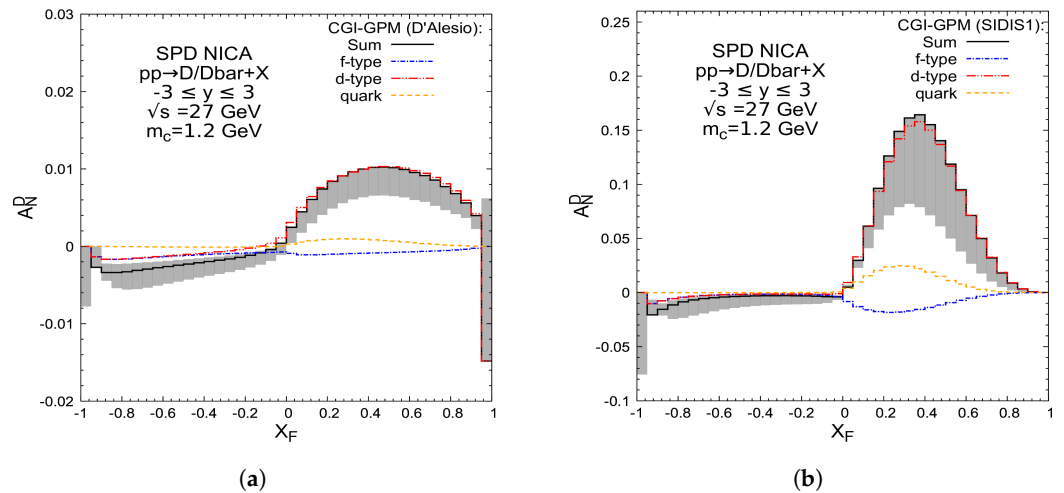
Figure 15. Estimated single transverse spin asymmetry of inclusive *D* meson productions at the SPD [25] using the colour gauge–invariant generalized parton model (CGI-GPM) for the two sets of the gluon Sivers function: (**a**) D'Alesio et al. [31] and (**b**) SIDIS1 [29].

High-precision measurements of the secondary vertex using silicon-based central trackers can help reduce the combinatorial random background. Figure 16a shows the relative sizes of the background and signal in the pion–kaon invariant mass spectra intended for D^0 decay reconstructions for one year of data at the SPD. Figure 16b illustrates the effects of the vertex detector in reducing the background. Monte Carlo simulation-based studies can reduce the background, and further improve the figure of merit by making the measurements viable to be compared to theoretical estimates.
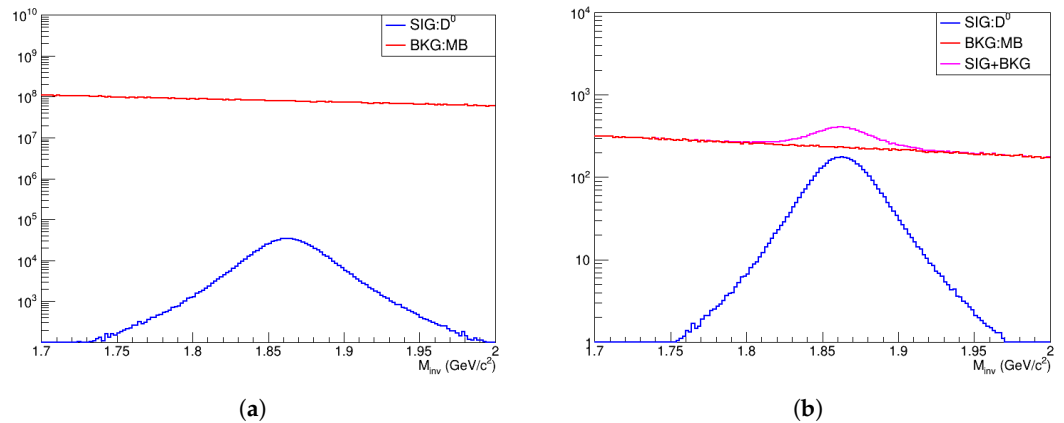

Figure 16. (**a**) Invariant mass spectra of random combinations of pions and kaons from the minimum bias (MB) data and those from D^0 decays for $x_F \geq 0.2$. (**b**) Selections based on the vertex detector used to suppress the combinatorial background. SIG and BKG denote the signal and background, respectively.

As can be observed from Figure 15, the two sets of parameters used to describe the gluon Sivers function in the theoretical calculations predict peak asymmetries differing by an order of magnitude [33]. The D'Alesio et al. parameters [31] predict asymmetries of the size of 1%, whereas SIDIS1 parameters [29] predict asymmetries of about 17%. SPD measurements can be extremely helpful in reducing such parameter dependence with a significant degree of statistical precision. From recent Monte Carlo studies on neutral *D* mesons, the projected statistical uncertainties of the single transverse spin asymmetries for one year of the foreseen data (Figure 17) show that measurements at the SPD are able to offer sufficient precision. These measurements have the potential to alleviate the significant model dependence observed in theoretical calculations and provide valuable data points for future extraction of the gluon Sivers function.
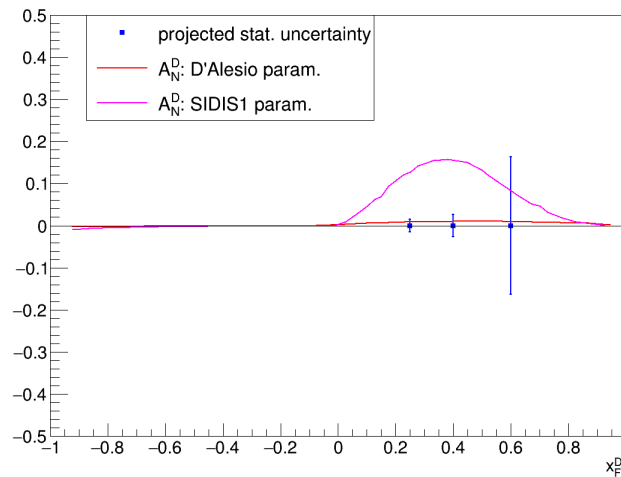
Figure 17. Projected statistical uncertainty of D^0 measurements at the future SPD for one year of data projected on estimated A_N of inclusive D mesons, calculated using D'Alesio et al. (red) [31] and SIDIS1 (magenta) [29] parameters of the gluon Sivers function.

3.4. Deuteron Measurements

The SPD is designed to serve as a unique laboratory to access information about the unpolarized and polarized structures of deuterons as it is considered to have the capacity to collide polarized deuterons over a range of energies.

Comparisons of unpolarized gluon PDFs of deuterons and protons (Figure 18a) show steep deviations above $x > 0.6$, indicating non-baryonic contributions. High-precision cross-section measurements at the SPD can be compared with theoretical calculations to test the predictions and the sizes of such deviations.
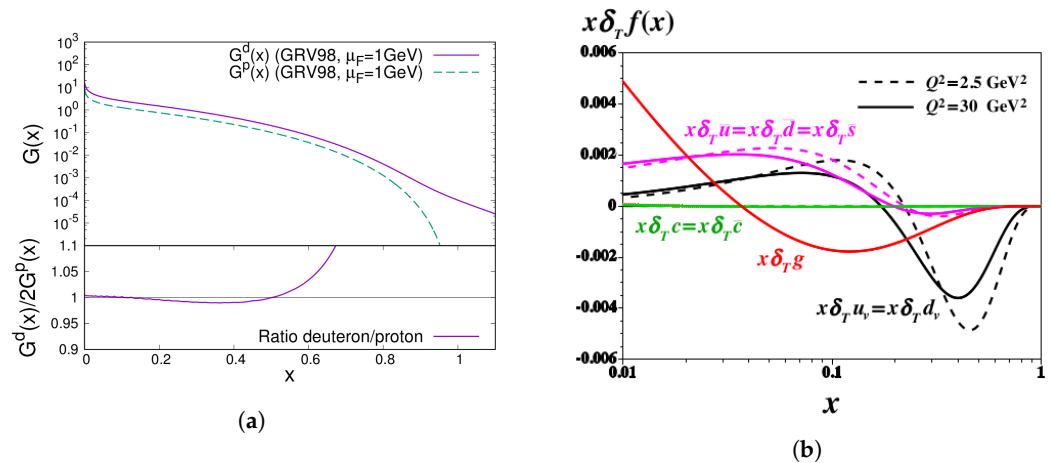

Figure 18. (**a**) Comparisons of the gluon contents of deuterons and protons inside deuterons [34]. (**b**) Tensor-polarized gluon PDF from the DGLAP energy evolution of quark/anti-quark PDFs [25].

Tensor polarization of quarks in deuterons has been formerly accessed via asymmetry measurements in DIS measurements by HERMES experiment [35]. However, according to Figure 18b, the DGLAP (Dokshitzer–Gribov–Lipatov–Altarelli–Parisi) energy evolution of PDFs suggests that at a higher energy scale, i.e., at $Q^2 = 30$ GeV), a non-zero tensor-polarized gluon component is possible. The vector and tensor single spin asymmetry measurements to be performed at the SPD are expected to be able to test such predictions from the perturbative QCD calculations.

4. Discussion

The SPD experiment at the NICA collider facility at JINR is poised to become a unique laboratory, offering a large variety of possible measurements from the collisions of polarized

proton and deuteron beams across a range of energies and luminosities. In the early stage of operations, measurements at the SPD will probe a wide range of interesting physics phenomena, encompassing spin effects in low-energy nucleon collisions, the formation of hyperons and hypernuclei, threshold production of charmonia, multi-parton scattering, and multiquark correlations. In the later stage of operations, the SPD experiment is planned to focus on its most prominent goal of accessing the gluon contents inside protons and deuterons via measurements of unpolarized cross-sections and various spin asymmetries in the production of different probe particles.

Physics programs at the SPD aim to test various phenomena at low-to-medium energies and provide high-precision data to improve the present understanding of nucleon structures, in general, and various spin structures, in particular. The results will help to test QCD in general, specifically focusing on providing data in a kinematic range that was not probed well to access the gluon content of the nucleons.

The results of the detailed Monte Carlo studies, presented in the current review for all three flagship channels of measurements at the SPD, are aimed at probing the gluon content of the nucleons.

For prompt photons, statistical reweighting techniques of PDFs illustrate the impact of helicity asymmetry measurements on the $\Delta g(x)$ for one year of the expected data at the SPD.

For charmonium (J/Ψ), the studies presented here illustrate the impact of the measurements of double-helicity asymmetries. For both measurements, the results demonstrate that the SPD will be able to significantly improve the knowledge of the helicity PDF in the large Bjorken-x region, as expected from the design and a proposal of the SPD.

For the open-charm channel, the studies presented in this paper shows significant improvements from the early designs by including the MAPS silicon detector as the central tracking device. The results presented here illustrate the effect of the high-precision secondary vertex reconstruction in significantly reducing the magnitude of combinatorial backgrounds by orders of magnitude. The statistical uncertainties of single transverse spin asymmetries are shown to be able to distinguish the severe model dependence observed in the description of the gluon Sivers function.

Fixed-target deep inelastic scattering experiments have estimated [36,37] separate Sivers and Collins contributions to the single transverse spin asymmetries but pp collider experimental results lack the precision to separate the two effects. For certain probes (i.e., meson production), the SPD is designed to allow investigations into the contributions of the Sivers and Collins effects in the single transverse spin asymmetries. A recent analysis [38] of TMD asymmetries measured in various SIDIS experiments (such as COMPASS and HERMES experiments) and on colliders (BRAHMS and STAR experiments) was attempted for the first time to extract the quark Sivers function. In Refs. [39,40], where the gluon TMD distributions and their contributions to the transverse spin asymmetry measurements of produced hadrons were studied, show the lack of experimental data in this budding field of interest. Attempts to extract the gluon Sivers distribution will require data from different kinematic ranges. At present, RHIC is the only pp collider capable of colliding polarized beams. In the future, the SPD is considered to be be able to provide some much-needed data for such phenomenological global analyses aimed at extracting gluon TMD distributions.

5. Conclusions

The SPD is an international Collaboration consisting of 32 institutes from 14 countries, encompassing about 300 members to date. The Collaboration is still growing and is open to participation from experts from all over the world.

The experiment's conceptual design report (CDR) [17] was published in early 2021 and was reviewed by the JINR Program Advisory Committee (PAC) in January 2022. Favorable reports from the PAC made it possible for the collaboration to move to the next step of producing a detailed technical design report (TDR) [26].

A tentative schedule anticipates the commencement of construction for the first stage of the detector in 2026, with the possibility of obtaining initial data around 2028. After a couple of years of data collection at lower energies and luminosities during the first stage of the physics goals, the SPD is scheduled to move to the next stage of upgrades with a focus on measurements accessing gluon components inside nucleons and light nuclei.

References

1. Ashman, J. et al. [European Muon Collaboration] A measurement of the spin asymmetry and determination of the structure function g_1 in deep inelastic muon-proton scatterin. *Phys. Lett. B* **1988**, *206*, 364–370. [CrossRef]
2. Adams, D.L. et al. [FNAL E704 Collaboration] Analyzing power in inclusive π^+ and π^- production at high x_F with a 200 GeV polarized proton beam. *Phys. Lett. B* **1991**, *264*, 462–466. [CrossRef]
3. Adams, D.L. et al. [FNAL E581/E704 Collaboration] Comparison of spin asymmetries and cross-sections in π^0 production by 200 GeV polarized antiprotons and protons. *Phys. Lett. B* **1991**, *261*, 201–206. [CrossRef]
4. Ellis, R.K.; Georgi, H.; Machacek, M.; Politzer, H.D.; Ross, G.G. Factorization and the parton model in QCD. *Phys. Lett. B* **1978**, *78*, 281–284. [CrossRef]
5. Collins, J.C.; Soper, D.E.; Sterman, G. Soft gluons and factorization. *Nucl. Phys. B* **1988**, *308*, 833–856. [CrossRef]
6. Ball, R.D. et al. [NNPDF Collaboration] A Determination of parton distributions with faithful uncertainty estimation. *Nucl. Phys. B* **2009**, *809*, 1–63; Erratum in *Nucl. Phys. B* **2009**, *816*, 293. [CrossRef]
7. Nocera, E.R. et al. [NNPDF Collaboration] A first unbiased global determination of polarized PDFs and their uncertainties. *Nucl. Phys. B* **2014**, *887*, 276–308. [CrossRef]
8. Ball, R.D. et al. [NNPDF Collaboration] The path to proton structure at 1% accuracy. *Eur. Phys. J. C* **2022**, *82*, 428. [CrossRef]
9. de Florian, D.; Sassot, R.; Stratmann, M.; Vogelsang, W. Evidence for polarization of gluons in the proron. *Phys. Rev. Lett.* **2014**, *113*, 012001. [CrossRef]
10. Glück, M.; Reya, E.; Stratmann, M.; Vogelsang, W. Models for the polarized parton distributions of the nucleon. *Phys. Rev. D* **2001**, *63*, 094005. [CrossRef]
11. Blümlein, J.; Böttcher, H. QCD analysis of polarized deep inelastic scattering data. *Nucl. Phys. B* **2010**, *841*, 205–230. [CrossRef]
12. Martin, A.D.; Stirling, W.J.; Thorne, R.S.; Watt, G. Parton distributions for the LHC. *Eur. Phys. J. C* **2009**, *63*, 189–285. [CrossRef]
13. de Florian, D.; Sassot, R.; Stratmann, M. Global analysis of fragmentation functions for pions and kaons and their uncertainties. *Phys. Rev. D* **2009**, *75*, 114010. [CrossRef]
14. Angeles-Martinez, R.; Bacchetta, A.; Balitsky, I.I.; Boer, D.; Boglione, M.; Boussarie, R.; Ceccopieri, F.A.; Cherednikov, I.O.; Connor, P.; Echevarria, M.G.; et al. Transverse momentum dependent (TMD) parton distribution functions: Status and overview. *Acta Phys. Polonica B* **2015**, *46*, 2501–2534. [CrossRef]
15. Sivers, D. Single-spin production asymmetries from the hard scattering of pointlike constituents. *Phys. Rev. D* **1990**, *41*, 83–90. [CrossRef]
16. Collins, J.C. Leading twist single transverse-spin asymmetries: Drell-Yan and deep inelastic scattering. *Phys. Lett. B* **2002**, *536*, 43–48. [CrossRef]
17. Abazov, V.M. et al. [The SPD Collaboration] Conceptual design of the Spin Physics Detector. *arXiv* **2021**, arXiv:2102.00442.
18. Hadjidakis, C.; Kikoła, D.; Lansberg, J.P.; Massacrier, L.; Echevarria, M.G.; Kusina, A.; Schienbein, I.; Seixas, J.; Shao, H.S.; Signori, A.; et al. A fixed-target programme at the LHC: Physics case and projected performances for heavy-ion, hadron, spin and astroparticle studies. *Phys. Rep.* **2021**, *911*, 1–83. [CrossRef]
19. Santimaria, M.; Carassiti, V.; Ciullo, G.; Di Nezza, P.; Lenisa, P.; Mariani, S.; Pappalardo, L.L.; Steffens, E. The LHC spin project. *SciPost Phys. Proc.* **2022**, *8*, 050. [CrossRef]
20. Willeke, F.; Beebe-Wang, J. (Eds.) *Electron Ion Collider Conceptual Design Report 2021*; Technical Report BNL-221006-2021-FORE; Brookhaven National Laboratory (BNL): Upton, NY, USA, 2021. [CrossRef]

21. Accardi, A.; Albacete, J.L.; Anselmino, M.; Armesto, N.; Aschenauer, E.C.; Bacchetta, A.; Boer, D.; Brooks, W.K.; Burton, T.; Chang, N.-B.; et al. Electron Ion Collider: The next QCD frontier. *Eur. Phys. J. A* **2016**, *52*, 268. [CrossRef]

22. Abramov, V.V.; Aleshko, A.; Baskov, V.A.; Boos, E.; Bunichev, V.; Dalkarov, O.D.; El-Kholy, R.; Galoyan, A.; Guskov, A.V.; Kim, V.T.; et al. Possible studies at the first stage of the NICA collider operation with polarized and unpolarized proton and deuteron beams. *Phys. Part. Nucl.* **2021**, *52*, 1044–1119. [CrossRef]

23. Goggi, G.; Cavalli-Sforza, M.; Conta, C.; Fraternali, M.; Mantovani, G.C.; Pastore, F.; Alberi, G. Inelastic intermediate states in proton-deuteron and deuteron-deuteron elastic collisions at the ISR. *Nucl. Phys. B* **1979**, *149*, 381–412. [CrossRef]

24. Richard, J.M.; Wang, Q.; Zhao, Q. Lightest neutral hypernuclei with strangeness −1 and −2. *Phys. Rev. C* **2014**, *91*, 014003. [CrossRef]

25. Arbuzov, A.; Bacchetta, A.; Butenschoen, M.; Celiberto, F.G.; D'Alesio, U.; Deka, M.; Denisenko, I.; Echevarria, M.G.; Efremov, A.; Ivanov, N.Y.; et al. On the physics potential to study the gluon content of proton and deuteron at NICA SPD. *Prog. Part. Nucl. Phys.* **2021**, *119*, 103858. [CrossRef]

26. Abazov, V. et al. [SPD Collaboration] Technical design of the Spin Physics Detector. *To be published*.

27. Brenner Mariotto, C.; Gay Ducati, M.B.; Ingelman, G. Soft and hard QCD dynamics in hadroproduction of charmonium. *Eur. Phys. J. C* **2002**, *23*, 527–538. [CrossRef]

28. De Florian, D.; Lucero, G.A.; Sassot, R.; Stratmann, M.; Vogelsang, W. Monte Carlo sampling variant of the DSSV14 set of helicity parton densities. *Phys. Rev. D* **2019**, *100*, 114027. [CrossRef]

29. D'Alesio, U.; Murgia, F.; Pisano, C. Towards a first estimate of the gluon Sivers function from A_N data in pp collisions at RHIC. *J. High Energy Phys.* **2015**, *119*, 1509. [CrossRef]

30. Karpishkov, A.V.; Saleev, V.A.; Nefedov, M.A. Estimates for the single-spin asymmetries in the $p^{\uparrow}p \to J/\Psi X$ process at PHENIX RHIC and SPD NICA. *Phys. Rev. D* **2021**, *104*, 016008. [CrossRef]

31. D'Alesio, U.; Flore, C.; Murgia, F.; Pisano, C.; Taels, P. Unraveling the gluon Sivers function in hadronic collisions at RHIC. *Phys. Rev. D* **2019**, *99*, 036013. [CrossRef]

32. Adolph, C. et al. [COMPASS Collaboration] Leading and next-to-leading order gluon polarization in the nucleon and longitudinal double spin asymmetries from open charm muoproduction. *Phys. Rev. D* **2013**, *87*, 052018. [CrossRef]

33. Karpishkov, A.; Saleev, V. On single transverse-spin asymmetries in *D*-meson production at the SPD NICA experiment. *arXiv* **2022**, arXiv:2212.07636.

34. Brodsky, S.J.; Chiu, K.Y.J.; Lansberg, J.P.; Yamanaka, N. The gluon and charm content of the deuteron. *Phys. Lett. B* **2018**, *783*, 287–293. [CrossRef]

35. Airapetian, A. et al. [HERMES Collaboration] First measurement of the tensor structure function b_1 of the deuteron. *Phys. Rev. Lett.* **2005**, *95*, 242001. [CrossRef]

36. Alekseev, M.G. et al. [COMPASS Collaboration] Measurement of the Collins and Sivers asymmetries on transversely polarised protons. *Phys. Lett. B* **2010**, *692*, 240–246. [CrossRef]

37. Alexeev, M.G. et al. [The COMPASS Collaboration] Measurement of P_T-weighted Sivers asymmetries in leptoproduction of hadrons. *Nucl. Phys. B* **2019**, *940*, 34–53. [CrossRef]

38. Cammarota, J. et al. [Jefferson Lab Angular Momentum (JAM) Collaboration] Origin of single-spin asymmetries in high-energy collisions. *Phys. Rev. D* **2020**, *102*, 054002. [CrossRef]

39. D'Alesio, U.; Murgia, F.; Pisano, C. Investigating the transverse momentum dependent gluon Sivers function in quarkonium production at *pp* colliders. *Few-Body Syst.* **2021**, *62*, 22. [CrossRef]

40. Boer, D.; Lorcé, C.; Pisano, C.; Zhou, J. The gluon Sivers distribution: Status and future prospects. *Adv. High Energy Phys.* **2015**, *2015*, 371396. [CrossRef]